

Promoting Healing Effect of Nano Material Bacterial Fiber on Sports Skin Wound

Yang Liu*

Institute of Problem, Dalian University, Dalian, Liaoning, China

liuyang@dlu.edu.cn

**corresponding author*

Keywords: Nano Materials, Bacterial Fibers, Sports Skin Trauma, Tissue Promoting Healing Effect

Abstract: Physical exercise is prone to cause various abrasions and the wound has no certain rules, prone to inflammation, slow healing and easy to form scars. Sports skin trauma is a major problem that plagues sportsmen. How to use effective methods to promote sports injury wound healing, reduce wound surface and shorten the course of disease is a problem worthy of discussion and research. This article analyzes the characteristics of sports wounds, skin structure and their effects on wound healing, and discusses the effects of nano-material bacterial fibers on sports wound healing. This article mainly conducts experiments from the effects of nano-material bacterial fibers on skin tissue's foreign body metabolism, growth catalysis, skin surface capacitance and surface gas exchange. Tissue samples in different chemical environments are set up. Experimental results show that the adsorption capacity of nano-material bacterial fiber is 50% higher than that of carbon fiber and polyester fiber, which can remove harmful bacteria on the skin surface to prevent inflammation in a short time. In skin tissues, bacterial fibers combined with zinc ions at a concentration of 0.5wt% can achieve the highest catalytic effect and promote cell regeneration and wound healing at the wound. When the contact concentration of the wound and the bacterial fiber is 4.5wt%, the wound can get the highest rate of oxygen, which can achieve the best healing effect.

1. Introduction

With the increasing pressure in people's lives, the backwardness of nanomedicine technology has become a major problem facing the medical industry today. Therefore, there is an urgent need to find nanomaterials that can relieve people's pain. In order to maintain health and reduce life pressure, countries are using legal means to attach great importance to the development of medical

nanotechnology. On the one hand, bacterial fiber waste is recycled and reused, on the other hand, bacterial fiber is used for research and development. Since 1980, the new nano-material bacterial fiber that can be degraded naturally has also become an important topic and has attracted worldwide attention.

Asadbegi M proposed the largest degradable plastic research program in the United States, which includes the development and research of the synthesis of degradable bacterial fibers, blending modification processing technology, and degradation experiments [1]. Karapolat S has successfully developed biodegradable nano-bacterial fibers. It has 5 sets of devices with an annual output of 45,400 tons, which can produce fully biodegradable bacterial fibers on an industrial scale [2]. Li Y developed a chemically and physically modified bacterial fiber nanomaterial Novon [3]. Jimenez F proposed that the oppositely charged layers formed on the interface between the electrode of the nano-bacterial fiber capacitor and the electrolyte are mutually exclusive [4]. Afterwards, El-Hoseny SM made supplements and improvements on the basis of this theory, proposed a double-layer bacterial fiber model, and proposed the concept of a diffusion layer [5]. Later, Peng X combined the charged solution theory with the double-layer bacterial fiber model theory and made a more detailed division to more accurately evaluate the performance of bacterial fibers [6]. Randy C discovered the electric double layer effect when preparing porous bacterial fiber materials and applied for the world's first patent on electrochemical supercapacitors [7]. Ferenc has developed thermoplastic nano-scale bacterial fibers and processed them into sheets and films with a tensile strength of 7-10 MPa and a breaking elongation of 150% to 230%. In terms of its appearance and performance, it can be used for disposable tableware and garbage bags, etc. It is currently improving its related performance and reducing costs [8]. In general, the current domestic research on biodegradable bacterial fiber is focused on biological tissue filling. From the perspective of the development of the entire biodegradable bacterial fiber, the production technology of bio-tissue filling is becoming more and more mature, and some products have begun to be industrialized. Photobiodegradation of bacterial fibers has attracted widespread attention and is one of the future development trends.

In order to develop a higher safety level of bacterial fibers, Lukanc B hydrolyzes bacterial cellulose through hydrochloric acid to produce a stable sol solution of nanoparticles [9]. The banana pseudostem fiber and bacterial cellulose are dispersed in a mixture of glycerin and distilled water, then starch is added and the mixture is heated until gelatinization occurs, and finally the mixture is cast and dried in an oven. This bioplastic is non-toxic and degradable and does not pollute the environment. The biodegradability of bacterial cellulose can also be used to add antibacterial materials in the process of synthesizing bacterial cellulose composite materials, which not only enhances the safety of the obtained food materials, but also ensures the environmental friendliness of the materials. The results show that the obtained nanoparticles are ribbon-shaped, with a diameter of 15-20nm, and a length ranging from 40nm to several microns. They show good hydrophilicity and lipophilicity, the sol solution shows great performance in delivering lipophilic biologically active substances. Nezhad MN uses modified coconut juice medium to cultivate G strain to obtain bacterial cellulose, which is then added to surimi to form a combined gel. This method improves the water holding capacity of surimi products and reduces the fat content of the products [10]. To overcome this problem, bacterial cellulose can be added to the glycerol-plasticized corn starch matrix and mixed with banana pseudostem fibers to form a mixed filler.

In this paper, the surface modification of nano-bacterial fibers with silicon coupling factor improves the dispersion ability of nano-bacterial fibers and is used in the healing of sports skin wounds. This paper conducts experiments from different angles to study the effect of nano-material bacterial fibers on the rate of foreign body metabolism in skin wound tissue, the degree of interference of bacterial cellulose on the capacitance of skin tissue, and the catalytic effect of

nano-material bacterial fibers on healing at a certain ion concentration.

2. Bacterial Fiber and Sports Skin Trauma

2.1. Aggregate Structure and Chemical Properties of Bacterial Fibers

The concentrated glucose ring of the nanobacterial cell unit has a strong reactive group, which makes it easy for molecular chains to aggregate and form a crystalline fiber structure. The cell fiber is a small stretching unit that forms the main structure of the cell, allowing long molecular chains to gather in a specific direction [11]. Due to the different methods of composition of plant cells and bacterial cells, the morphology of plant cells and bacterial cells are also different. First, the cell structure on the plant cell wall is its skeleton, embedded in a matrix composed of cysteine, pectin and certain proteins, surrounded by lignin. Bacterial cellulose is not a structural component of bacterial cell walls, but a product secreted by extracellular bacteria [12]. It is an independent fiber, cellulose produced by a single glucose concentration, and its content is extremely high, not mixed with other polysaccharide impurities such as lignin and semi-nitrate. The microcatheters of the two are also different: the bacterial cell is first formed by a glucose chain with a width close to 1.5nm, and the welding of naturally formed fibers with hydrogen forms a fibrous compound. The fibers are assembled into bundles and then form a shaped structure [13]. The cell synthesis rate of bacteria is very high. Any kind of acetobacter xylinum can polymerize 150 million glucose molecules per hour and can produce at least 11.83 tons of cellulose, unparalleled cellulose formed by the photosynthesis of green plants [14].

The polymer structure of histatin is to study the mutual combination of cellulose molecules. The basis of studying the polymer structure of cellulose macromolecules is to master various crystal variants in the crystal structure of tissue element [15]. Studies have shown that there are five crystalline variants of cellulose, namely tissue element I (natural tissue element), artificial tissue element II, and IHI. When studying the different sources of histatin I, it was found that the parameters of these histatins are slightly different. Therefore, the cellulose is divided into IA histatin and IB histatin. Each IA histatin has a tricyclic crystal structure. IB histidine has two single histidine chains. For example, bacterial cellulose contains 60% IA and 40% IB, while cotton, hemp and other plants have only 30% IA and 70% IB. The IB type histogen is irrevocable after hydrothermal treatment of cellulose. This may be because type BC is a chemical derivative and an important reason for its sensitivity to cellulose [16]. The four main variants of histidine have almost the same molecular chains, and their main difference lies in the formation of histidine. The transformation and transformation of histatin crystals can be divided into two categories: histatin cluster I and histatin cluster II. The main difference between the two is the direction of molecular chain formation. The tissue element I is located in the parallel chain, and the tissue element II is located in the parallel chain [17]. The crystalline modification of the tissue element may undergo some changes, but none of the crystalline state is transformed into the dispersed state of the unit cell. The unit cell structure is divided into two parts: the crystalline region and the amorphous state. The unit cell structure is divided into two parts, the crystalline region and the amorphous state. The percentage of the crystal plane in the whole unit cell is called the crystalline substance of the unit cell. As the purity of the crystal increases, the resistance to external forces increases, the bulk modulus, hardness, specific gravity and stability of the fiber are reduced, while the elongation, moisture, swelling, softness and chemical reactivity are reduced. It is higher than pure fine plant fiber, but lower than algae and animal fiber. However, the humidity, magnification, softness and chemical reactivity of bacterial tissue elements are much better than those of higher plant tissue elements. The abnormal phenomenon caused by the extremely fine network structure.

Compared with plant cellulose, tissue cellulose can be obtained without lignin and original

cellulose, and the purity can reach more than 90% after simple extraction. Tissue cellulose is composed of 4 nanometer microfibrils, which are wound into ribbons through hydrogen bonds between cellulose molecules. As far as the diameter of the fiber section is concerned, tissue cellulose is very different from plant fibers, and its diameter is only cotton one percent of fiber [18]. Due to the ultra-fine nanomaterials of bacterial cellulose, its surface area is 250 times that of lignocellulose, and the large amount of hydrophilic on the surface of biocellulose nanofibrils endows tissue cellulose with high absorption, water retention and water retention properties. In this case, it can absorb water 60-700 times its own weight, and can be used in the field of water-absorbing materials.

Bacterial cellulose can be adjusted in the process of biological problem environment stabilization. For example, acetobacter can synthesize N-acetylglucosamine from glucose and acetylglucosamine, and combine N-acetylglucosamine with bacterial cellulose at a ratio of 4%. For example, the addition of carboxymethyl cellulose, methyl cellulose or polyvinyl alcohol (PVC) in the medium will change the structure, crystal shape and water content of BC, as well as its ability to absorb metal ions. Bacterial cell membranes with Young's modulus can obtain higher tensile strength and excellent shape retention by using different culture methods, such as static fermentation of acetobacter. Bacterial cells are high molecular polymers produced by acetobacter. High biocompatibility, almost no foreign body and inflammatory response, and good mechanical resistance to fluid conditions, which makes it suitable for fabric manufacturing materials. It has specific applicability. At the same time, bacterial cellulose can be physically degraded under the action of microorganisms and cell catalysts without polluting the environment.

2.2. Sports Skin Trauma

Sports skin trauma refers to injuries that occur during sports training and daily activities. During exercise, due to unbalanced center of gravity, external impact, technical errors, improper force, etc., sports injuries may occur. It is different from the injuries that occur in general production labor, transportation and daily life [19]. Sports trauma wounds often exhibit irregular wound edges and incompatible features. Depending on the degree of trauma, it may also be accompanied by some tissue damage, rupture of blood vessels and destruction of bone structure. When tissue integrity is damaged, a wound is formed, and healing is the process of restoring tissue integrity. Sports trauma is characterized by a long period of illness, slow healing of the wound, and easy scar formation. Mild wounds are limited to the surface of the skin, more severe ruptures in the skin and deeper layers, severe wounds may include rupture of skeletal muscles, tendons, and sensory lines. The time of wound healing and the quality of healing are also issues that need to be actively addressed after sports injuries occur, which are affected by many factors [20]. In skin anatomy, the skin is composed of the epidermis, dermis and subcutaneous tissue, and each layer plays an important role in maintaining skin health. The epidermis is located on the top of the skin and its function is to regenerate cells and metabolism. The dermis is located in the central layer of the skin and contains collagen to make the skin more elastic, increasing flexibility and adaptability. The skin also contains microscopic blood vessels, nerves, hair follicles, sweat glands and glands with mold. The subcutaneous tissue is a layer of fat that protects the upper layer of cells and provides an adjustable external solution. The skin plays an important protective role during exercise. During the formation and healing of skin trauma, sports injuries may cause skin damage to reach the subcutaneous tissue. The healing process of skin wounds is a process of gradual repair of the skin layer. When the integrity of the tissue decreases, the wound is formed. Healing is the process of restoring tissue integrity, and wound healing is common. Therefore, in the process of sports wound skin wound healing, the steps of hemostasis, inflammatory response, regeneration and tissue reconstruction are

also performed [21]. After the wound is created, tissue necrosis, blood vessel rupture and bleeding will occur around the wound to varying degrees. The process of hemostasis is the first process after trauma. In the process of hemostasis, the chemokines, cytokines, growth factors, and hypoxic environment in the wound stimulate neutrophils and monocytes, macrophages and lymphocytes travel through blood vessels to reach the wound site.

2.3. Surface Modification of Nano-Material Bacterial Fiber

Interface is a key component of nanomaterials, and it is also a key technology that limits the performance of nanomaterials. Whether the matrix material and the reinforcing fiber are infiltrated and well bonded directly affects the load transfer efficiency in the composite material [22]. Macroscopic properties are the mechanical properties of composite materials. In the early days, people used glass fibers to reinforce resin-based composite materials, and found that when the material was exposed to a humid environment for a long time, the strength would be greatly reduced. Due to the intrusion of water molecules, the resin is debonded from the hydrophilic glass fibers, which is the main cause of strength loss. Bacterial cellulose is a hydrophilic fiber, and its surface functional group is group, which has a strong affinity for water molecules. The resin material is mainly a hydrophobic ester functional group, which cannot form a good bond with water. Therefore, when preparing fiber-reinforced resin-based composite materials, the surface of the fibers must be modified. The hydrolysate of the coupling agent reacts with the groups on the fiber surface on the one hand, and chemically combines with the resin matrix on the other hand. Chemical bonding occurs at the interface of the composite material to connect the fiber and the resin matrix, thereby improving the performance of the composite material [23].

2.4. Capacitiveness of Nanometer Bacterial Fiber

The capacitive properties of nano-bacterial fibers are called electrochemical capacitors. On the one hand, they have the high energy storage of batteries and lithium batteries. On the other hand, they can also meet the high-power charging and discharging characteristics of capacitors. They have double-layer capacitors and pseudo there are two types of capacitor mechanisms. Electronic materials are the key to determining the efficiency of the supercharger. The high specific surface area and high active material of the electrode will significantly improve the performance of the supercharger. The load passes through the electric double layer at the interface between the electrode and the electrolyte. The pseudocapacitance is the redox of the active material in the capacitor electrode produced by a fast reversible reaction. The main point is that there are two interactions between the electrode and the electrolyte, one is electrostatic interaction. The other is the short-range interaction between ions, such as van der Waals forces, unipolar bonds, etc. [24]. These two effects make the oppositely charged particles tend to align close to the surface of the electrode material, forming a dense layer. Because of the molecular thermal movement, the electrolyte particles cannot completely adhere to the electrode and have a certain degree of dispersibility, forming a dispersed layer, and the entire single electrode forms an electric double layer structure. Energy is stored on the surface of the electrode material in the arrangement of ions. When charging, the external power supply provides electrons to enter, so that the metal ions in the solution repel each other and move to the vicinity of the power supply under the force of the electric field. Discharge is the opposite movement of electrons, positive and negative ions. The calculation formula of specific capacitance is:

$$C = \varepsilon \times S / d \quad (1)$$

Among them, C is the capacitance, ε is the electrolyte system, S is the size of the electrode block, and d is the minimum distances between the metal ions that can approach the electrode block [25]. Generally speaking, under the same electrolyte conditions, since the thickness of the dielectric layer of the double layer depends on the ionic radius and other factors, the super capacitor of this mechanism is generally made of materials with high specific surface area to obtain a larger specific capacitance and storage capacity. Pseudocapacitance also called Faraday quasi-capacitors, usually use transition metal oxides or conductive polymers. In the case of the same specific surface area, due to the interaction of the electrostatic charge and the redox reaction, the pseudocapacitance can obtain a higher tissue density than the electric double layer capacitor. For conductive nanomaterials, it is mainly through the two doping and dedoping mechanisms of P and N to achieve charge transfer to achieve the purpose of energy storage. The formula for calculating the energy storage of pseudocapacitors can be referred to as follows, where F is a constant, n is the number of charge transfers, M is the molar mass, and V is the potential window:

$$c = n \times F / (M \times \nabla V) \quad (2)$$

At present, the limited source and high capital cost of transition metal oxides as pseudocapacitance electrode materials limit their development and use. Conductive polymers also have many problems in terms of controllable synthesis and long cycle life. Relatively speaking, the development of pseudocapacitors needs more exploration. In addition to the symmetric supercapacitors with the same two electrode materials, there are also asymmetric devices and hybrid devices with different electrode materials or even different mechanisms [26]. In symmetrical devices, the main problem is to solve the voltage limitation of the aqueous electrolyte. Recently, it has been reported that symmetrical devices with dual activated carbon electrodes have been able to reach a working voltage of 1.6V in a neutral electrolyte, and long-term use is guaranteed. The voltage of dual-carbon material symmetrical devices has been further expanded in the aqueous electrolyte rich in lithium ions. Asymmetric supercapacitors generally have an electric double layer mechanism electrode and a pseudocapacitance material, such as AC/MnO₂, which can be reversibly cycled between 0 and 1.5V in an aqueous electrolyte potassium sulfate solution. The energy density is 10Wh/kg and the power density 3600W/kg. Hybrid capacitor devices are generally composed of two electrode materials with different mechanisms (such as electric double layer type and intercalation type). At present, the mainstream and most researched are mainly activated carbon and graphite.

2.5. Preparation Method of Nano Bacterial Cellulose Adsorption Aerogel Composite Material

Through physical blending or chemical modification, the adsorption and enrichment of heavy metal ions by BC can be further enhanced, and the metal ions obtained by adsorption can be used to enhance electrochemical performance. It mainly includes the preparation of PVA/BC composite aerogel and the preparation of amino-modified bacterial cellulose aerogel, as well as subsequent adsorption experiments and pyrolysis carbonization steps [27]. The specific experimental process is as follows: the bacterial cellulose is cleaned and dispersed, and the steps are the same as the dispersion treatment process in experiment 1. Prepare PVA solutions of different concentrations (4/10/20mg/ml), mix and stir 1ml PVA solution with 10ml of the above BC dispersion liquid. In order to ensure uniform mixing, process in a hot environment (80 °C) for 3h to obtain a mixed slurry. Freeze-dried for 24h to obtain PVA/BC composite aerogel. The sample is marked as PVA/BC-x (x is the number of parts by mass of BC when PVA is one part by mass). Take 200mL of BC dispersion and add 4g NaOH solution to make it alkaline reaction environment, add 6mL epichlorohydrin, stir and react at room temperature for 1 hour, take out centrifugal cleaning to pH neutral for use. The

above product was re-dispersed to 200ml with deionized water, 1g of sodium bicarbonate was added, 5g of ethylenediamine was added after stirring, stirred for 2h, centrifuged, washed, and freeze-dried to obtain the final product. The sample is labeled EDA-BC. Take 10mg of the above-mentioned materials and place them in 50mL CuCl₂ solution with a concentration of about 5mg/L. After adsorbing for 24h, take a little adsorption solution after 48h for testing. The test method follows GB/HJ485-2009 with a little improvement. The above-mentioned material after adsorption of copper ions was dried, and carbonized and pyrolyzed at 700 °C in a nitrogen atmosphere at a heating rate of 5 °C/min for 2 hours. The materials were divided into two groups, one group was directly subjected to electrochemical characterization, and the other group was performed at 200 °C air environment oxidation treatment for 20 hours, and then purification.

3. Experimental Design of Promoting Effect of Bacterial Fiber on Sports Skin Trauma

3.1. Preparation of Experimental Objects

This experiment studies the effects of nano-material bacterial cellulose on the acidity and alkalinity, catalytic properties, capacitance and air contact area of skin wound tissue under different environments. Utilize the multi-level cultivation method combining up and down to prepare multi-level bacterial tissues with similar quality. The composite material of bacterial cellulose and hyaluronic acid (HA) with different concentrations was prepared by solution immersion method. The physical and chemical properties of the composite material were characterized by scanning electron microscopy (FE-SEM), and primary human skin fibroblasts were planted on the material for cell evaluation.

3.2. Experimental Plan Design

(1) Experimental Environment Design

Before the experiment of bacterial cellulose on sports skin trauma, the cultured bacterial cellulose needs to be washed and lyophilized. Wash the bacterial cellulose soaked in the NaOH aqueous solution with ultrapure water several times until it is neutral. After treatment with liquid nitrogen, it is put into a freeze dryer and freeze-dried. When the bacterial fiber contains no moisture, it is taken out for use. The prepared bacterial cellulose maintains the macroscopic morphology in the wet state without significant volume changes. Place the freeze-dried bacterial cellulose in a tube furnace, set a certain temperature rising curve, and perform carbonization at 800 °C and 1200 °C under a protective atmosphere of pure argon, thereby preparing carbon nanofibers. The amount of carbon nanofibers prepared at 800 °C is relatively large for subsequent graphitization. The samples carbonized at 800 °C were placed in a high-temperature graphitization furnace, and graphitized at three different temperatures of 2200 °C, 2600 °C, and 2800 °C under a protective atmosphere of pure argon.

(2) Experimental Steps

Because the chemical environment of sports skin wounds is unstable during the healing process, the optimal pH and initial concentration are selected for the experiment of bacterial fiber adsorption of harmful ions to study the ability of bacterial fiber to adsorb metabolic waste. A certain amount of bacterial fibers are respectively packed in the three adsorption columns and soaked in secondary deionized water for a certain period of time. The prepared manganese solution with a concentration of 0.1mg/L (or a chromium solution with a concentration of 1.1mg/L) flows through a gravity column with a diameter of 2.0cm from top to bottom, and the resulting solution is collected at regular intervals and used atomic spectrophotometry meter measures the concentration of Ar (or Mn) ions in the effluent. When the concentration of the effluent is about 95% or more of the

concentration of the influent, it can be determined that the adsorption is saturated. The maximum adsorption capacity is an important indicator to describe the adsorption capacity of a material. The model is used to fit the column adsorption process to obtain the maximum adsorption capacity. The formula of Thomas model is:

$$\frac{C_e}{C_0} = \frac{1}{1 + \exp\left(\frac{k}{Q}(q_0M - C_0V)\right)} \quad (3)$$

Among them, C_e is the concentration of cadmium ions in the resulting solution(mg/L); C_0 is the initial concentration of cadmium ion(mg/L); k is basic constant(ml/min/mg); q_0 is the maximum adsorption capacity(mg/g); M is the weight of the adsorbent(g); V is the volume of solution flowing through the adsorption column within a certain period of time(ml); Q is the flow rate(ml/min). Convert equation (1) to get the linear form of model:

$$\ln\left(\frac{C_0}{C_E} - 1\right) = \frac{kq_0M}{Q} - \frac{kC_0V}{Q} \quad (4)$$

3.3. Statistical Methods

For the healing promoting effect constitutive model, the test rising scheme of the healing promoting effect can be a square or cubic equation, and the descending segment is a logical component model, which is the most representative and globally recognized component model of various forms. These two models include the following content, where a_0, a_1, a_2, a_3 and b_0, b_1, b_2 all represent undetermined coefficients. The first model:

$$\begin{cases} y = a_0 + a_1x + a_2x^2 + a_3x^3 & x \leq 1 \\ y = \frac{x}{b_0 + b_1 + b_2x^2} & x \geq 1 \end{cases} \quad (5)$$

In the second model, the rising and falling sections are the same equation, but the parameters in the equation are different. $A_1, A_2, B_1,$ and B_2 are undetermined coefficients.

$$y = \frac{A_1 + B_1x^2}{1 + A_2x + B_2x^2} \quad (6)$$

4. Promoting Effect of Nano-Material Bacterial Fibers on Sports Skin Trauma

4.1. Absorption Ability of Bacterial Fiber to Wound Foreign Body

As shown in Figure 1, as the carbonization temperature rises, the position of the bacterial fiber adsorption peak shifts to the right. After 100 minutes, the adsorption capacity of bacterial fiber is 1.4 units, which is 50% higher than carbon fiber and polyester fiber. At 500 min, the adsorption peak is at the maximum limit, but the angle at which the 400 min peak is located does not change significantly, indicating that the adsorption capacity of bacterial fibers reaches the maximum at 400 min, and the protection task in human tissue has been completed. The calculated results of the polyester interlayer spacing show that only after high temperature graphitization, the interlayer

spacing of the samples is between 0.2-0.6, while the carbonized bacterial fiber layer has a larger spacing. Therefore, as the temperature increases, the degree of adsorption of the obtained nanobacterial fibers to biological tissues will increase. When polyester is present, the ability of bacterial fibers to adsorb cadmium is significantly lower than that of bacterial fibers without polyester. The Thomas model is used to fit the data. The results show that when arm is alone, the maximum adsorption capacity of bacterial fibers is 23.65mg/g, but when there is polyester, the maximum adsorption capacity of the material for arm drops to 18.70mg/g. This may be because when polyester exists alone, polyester can only adhere to the position with higher adhesion energy, when polyester and Ar coexist, adhesion sites with lower adhesion ability can also adhere to polyester. The number of adhesion sites on the surface of bacterial fibers is certain. When lead occupies more adsorption sites, the adsorption capacity of bacterial fibers for arm will inevitably decrease.

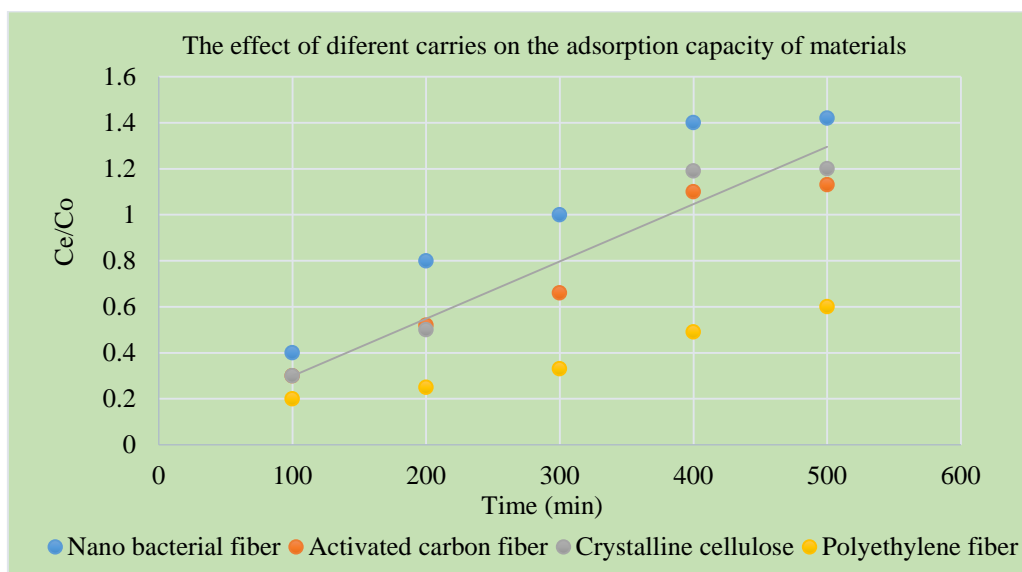


Figure 1. The effect of different carriers on the adsorption capacity of materials

4.2. Catalytic Properties of Nano-Material Bacterial Fibers

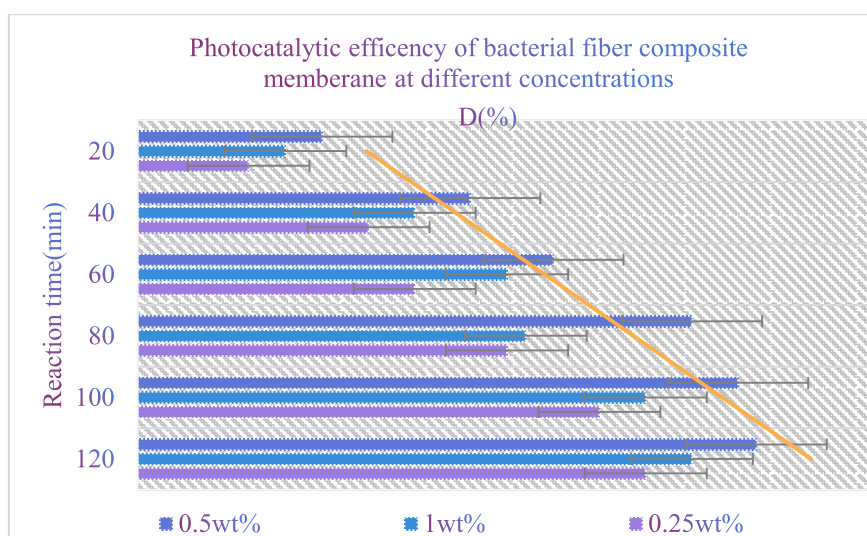


Figure 2. Photocatalytic efficiency of bacterial fiber composite membrane at different concentrations

As shown in Figure 2, the photocatalytic efficiency of the nano-bacterial fiber composite membrane obtained under different zinc ion concentration preparation conditions on the methyl orange solution. The results show that the bacterial fiber composite membrane obtained under the condition of 0.5wt% zinc ion concentration has the highest photocatalytic efficiency, reaching 70% at 2h, and the performance of the bacterial fiber composite membrane obtained under the conditions of 1wt% and 0.25wt% concentration is second. The photocatalytic activity of the nano-bacterial fiber composite membrane is affected by the loading of ZnO nano-bacterial fiber, particle size and specific surface area. When the zinc ion concentration is 0.25wt%, SEM and thermal weight loss analysis show that the ZnO nanobacterial fiber loading in the composite film is about 2%, and the low ZnO loading results in its lower photocatalytic efficiency. When the concentration of Zn^{2+} increased to 0.5wt%, the particle size of ZnO nanobacterial fibers was maintained at about 50nm, and the distribution was uniform. Thermogravimetric analysis showed that the content of ZnO nanoparticles was increased to 6%, so the photocatalytic efficiency was significantly higher. However, further increasing the concentration to 1wt% will further increase the particle size of ZnO nanoparticles, reduce their specific surface area, and increase the content of ZnO nanobacterial fibers by only 1.4%. The smaller the size of the ZnO nanoparticles, the larger the specific surface area, and the higher the photon absorption capacity, thereby significantly improving the photocatalytic efficiency. Therefore, the composite film obtained at a concentration of 0.5wt% has the highest photocatalytic activity.

As shown in Table 1, the contact area of skin wounds healed by the catalyst BH-P/BC and air is significantly larger than that of CH-R/BC, because the activity of sodium borohydride in reducing platinum particles is higher than that of formaldehyde. The two catalysts, BH-R/BC and HC-PU/BC, showed an obvious redox peak between 0.4V and 0.6V. This peak should be attributed to the oxidation and reduction of oxygen-containing groups on the cellulose surface. In the study of polymer-supported Pt as a catalyst, the oxygen-containing groups on the polymer surface have the same peaks formed by redox. Using the low-potential part (-0.2V-0.1V) of the cyclic voltammogram, the desorption peak area of hydrogen can be used to calculate the amount of electricity (QH) and the relative electrochemical active area (EAS) is $24.6m^2/g$. QH is the amount of electricity required to adsorb hydrogen on the surface of R. It is calculated by the electrochemical activity of hydrogen on the surface of R. The EAS $34.8m^2/g$ of the catalyst reduced by sodium borohydride is much higher than the EAS-21 of the catalyst reduced by formaldehyde $4m^2/g$, this experimental result confirms that the catalyst reduced by bacterial fibers is more suitable as a catalytic layer for sports skin wounds.

Table 1. Comparative analysis of electrochemical active area of common catalysts

Sample	Reducing agent	The average particle size	EAS(m^2/g)
BH-R	$NaBH_4$	3.3	34.8
HC-PU	HCHO	3.9	21.4
BH-R	$NaBH_4$	14.7	31.3
HC-PU	HCHO	17.8	16.4
BH-R	CH_2OHCH_2OH	4.5	24.6
HC-PU	CH_2OHCH_2OH	4.5	41.1
BH-R	CH_2OHCH_2OH	2.4	65.3

4.3. Influence of Bacterial Fibers on the Gas Exchange Skin Surface

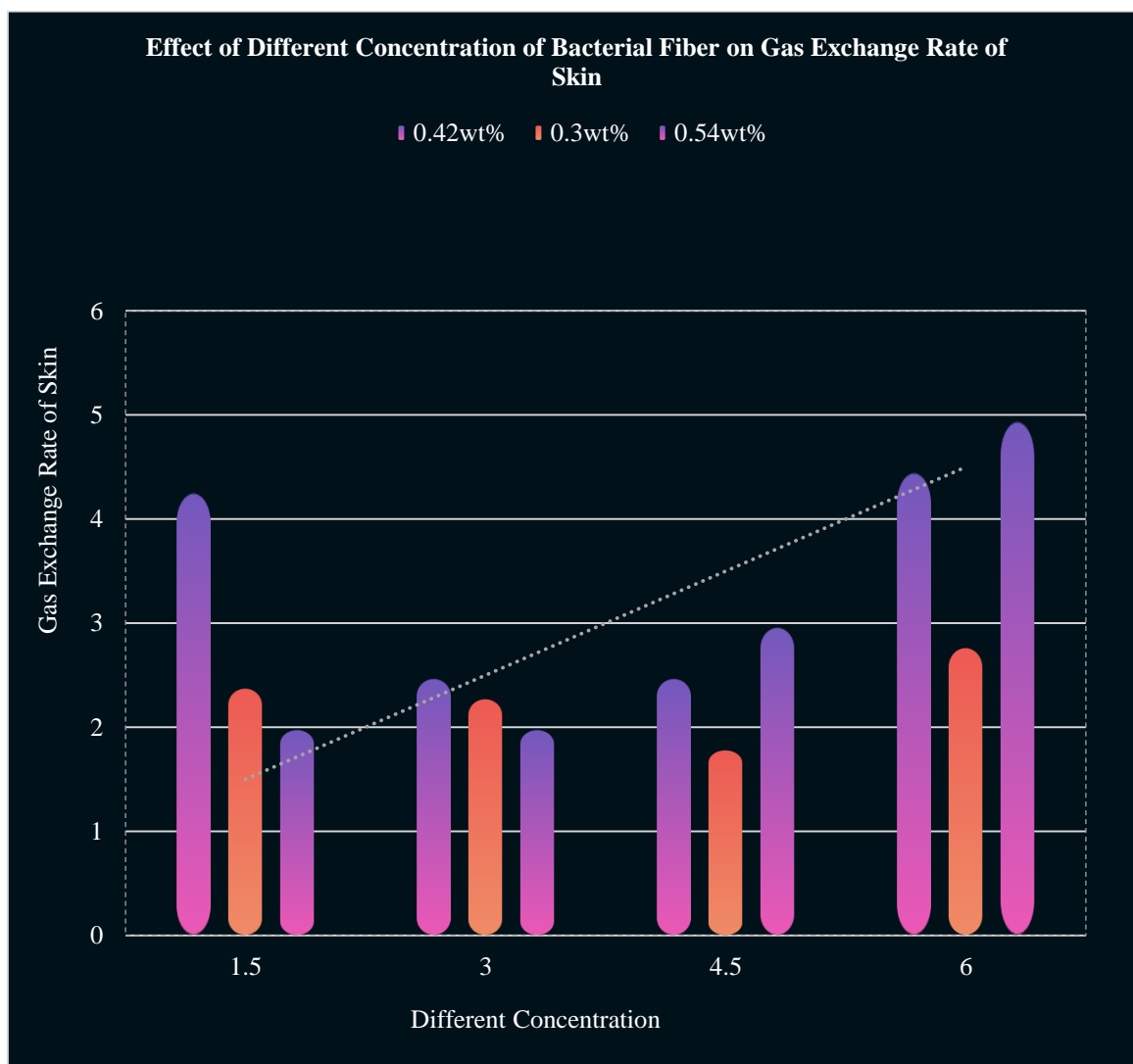


Figure 3. Effect of different concentration of bacterial fiber on gas exchange rate of skin

Attention should also be paid to the phase separation of the BC nano-aqueous suspension obtained by the hydrolysis of sulfuric acid. The separation of the suspension at a concentration of 0.42wt% or more has an isotropic and chiral liquid crystal phase with obvious phase boundaries. The order domain size in the anisotropy stage decreases with the concentration of NaCl ranging from 0 to 2.75 wt%. In this entire range, up to 2.75wt%, semi-crystals can be observed, and when the concentration reaches 5.0wt%, the chiral liquid crystal field is no longer observed. As the concentration of NaCl increases, the spacing of chiral liquid crystals decreases, reaching the lowest value at about 0.75 wt%, and then when the concentration of NaCl reaches 2.0 wt%, the spacing of chiral liquid crystals increases sharply. When preparing a neutral bacterial cellulose nano-smooth model surface, obtaining a good dispersion suspension is a prerequisite. However, the neutral nano-suspension will have obvious particle aggregation. Adding carboxymethyl cellulose or xyloglucan to the polymerized BCN suspension can minimize this problem. CMC increases the dispersion concentration ratio of BCN to more than 0.05wt%. In the case of XG, the colloidal stability is enhanced, and the observed concentration ratio is more than 0.5wt%. The results

obtained show that the cellulose-based model surface can be obtained by spin coating using CMC/BCN or XG/BCN method, which exhibits a more uniform morphology than the unmodified BCN reference model surface and surface roughness.

When the contact concentration is 4.5wt%, the healing effect of bacterial cellulose is the best. It can be seen that when the contact amount is low, as the contact amount increases, the implantation speed of cellulose increases faster. In the case of low exposure, due to the small number of acetobacter xylinum, almost all strains can effectively produce cellulose. The amount of bacterial cellulose produced by metabolism in the same time increases with the increase of the inoculum; when the amount is higher, the yield of cellulose decreases with the increase of the inoculation amount. Acetobacter xylinum is a strict aerobic bacteria. In the case of a large amount of inoculation, the number of bacteria in the solution increases, which consumes O_2 and nutrients there are more, and the oxygen and nutrients in the fermentation broth are limited, causing many bacteria to die due to insufficient oxygen and nutrition, which affects the synthesis and secretion of bacterial cellulose.

4.4. Influence of Bacterial Fibers on the Capacitance of Skin Tissue

Cyclic voltammetry can detect the nutrient-oriented voltage of the nano-material bacterial fiber during the healing process of sports skin wounds. The longer the test time, the more voltage data can be obtained and theoretical discussion can be conducted. Recursive voltammetry is a basic method often used in electrochemical measurements.

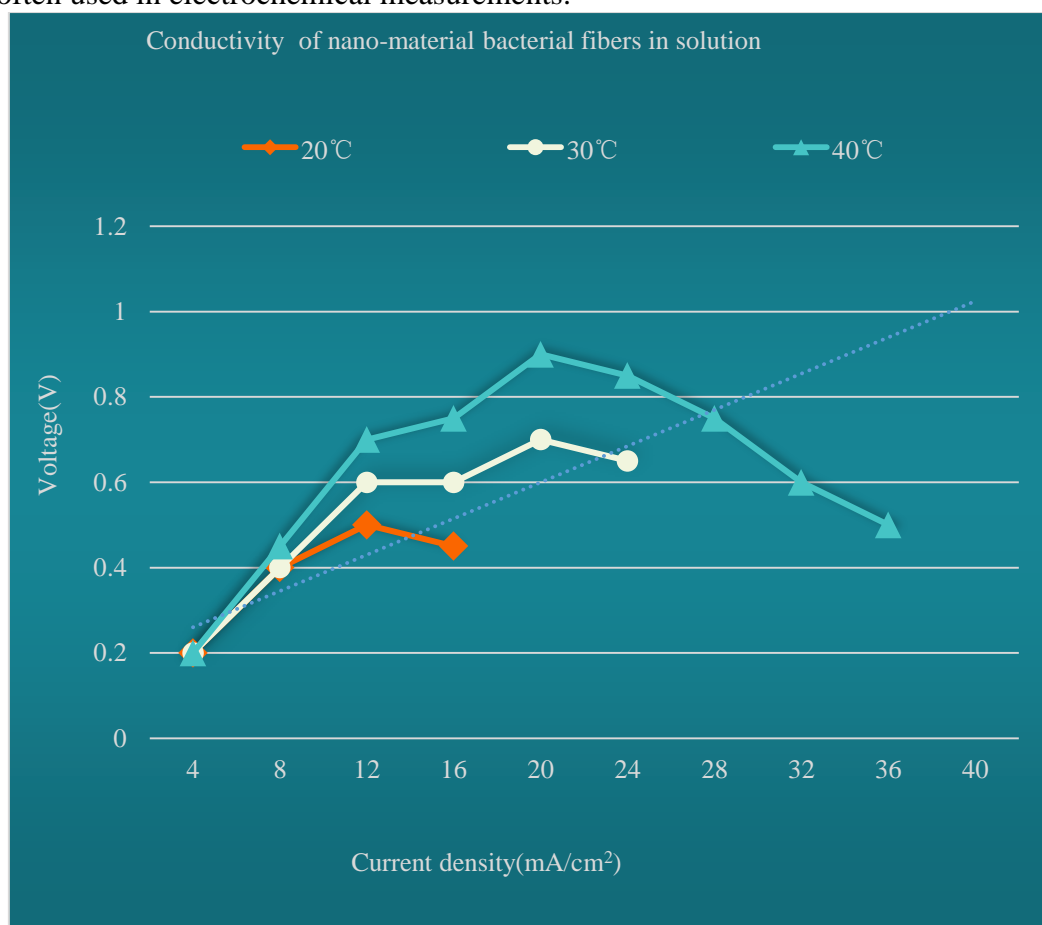


Figure 4. Conductivity of nano-material bacterial fibers in solution

As shown in Figure 4, the conductivity of HOP bacterial fiber and tungstophosphate-doped nanomembrane catalyst to human tissue fluid at different temperatures (20, 30 and 40 °C), the operating condition is 0.02MPa, the human body's utilization of bacterial fibers 90%, air utilization rate 40%. It can be seen from the figure that normal pressure dry hydrogen and dry air are used as catalysts and oxidants, and the performance of the PWA-doped BC membrane self-humidifying fuel cell increases with the increase in temperature (20 to 40 °C). This is due to The electrochemical reaction speed (kinetic factor) of nano-material bacterial fibers increases with the increase of temperature. The battery performance and output performance of the bioconductor assembled by the commercialized bacterial fiber catalyst and the tungstophosphate-doped nanomembrane under the same test conditions is slightly better than the output performance of the self-made catalyst assembly battery. The peak specific power of the self-humidifying bioconductor prepared by the self-made catalyst and the commercial catalyst reached $12.1\text{mA}/\text{cm}^2$ and $17.9\text{mA}/\text{cm}^2$, and the open circuit voltage was 0.2V and 0.92V, respectively. The open circuit voltage of the bioconductor prepared by the hydrophilic bacterial cellulose-supported catalyst is nearly 40mV higher than that of the bioconductor prepared by the Pt/C catalyst, which shows that the BH-R/BC catalyst has the ability to inhibit gas crossover and reduce oxygen. The polarization of the electrode eliminates the effects of mixed potential and short-circuit current. The maximum output power of the biological conductor prepared with bacterial cellulose loaded R is 1.45 times that of the ordinary conductor. It is speculated that the reason for the improved performance of human tissue conductors is the increased proton conductivity of the bacterial cellulose membrane after proper treatment.

5. Conclusion

Graphite oxide nanosheets are introduced into bacterial cellulose and reduced by glucose to give the composite nanomaterials conductivity. The effect of different composite methods on the properties of composite nanomaterials is discussed. For in-situ compounding, methods such as adjusting the value during the cultivation process and adding the suspension in batches can be considered to control the flocculation of the particles during the cultivation process. For composite nanomaterials prepared by the immersion method, centrifugation can be used to screen nanosheets with a smaller particle size, combined with ultrasound, to prepare composite nanomaterials with a more uniform structure.

Nano-material bacterial fibers play a very good effect in the healing process of sports wounds. Bacterial fibers can stimulate proliferation factors. Proliferation factors are a class of biologically active peptides that promote cell differentiation. They play a key role in wound healing, including NGF and TGF. NGF can not only promote the growth and development of nerve cells, enhance the innervation of sensory nerves in keloids, but also have a chemotactic effect on immune cells and promote the release of other cytokines. The mechanism of action of traditional Chinese medicine is mostly related to the growth factors that can stimulate wound healing. The anti-inflammatory effect of curcumin can also be linked with the inflammatory response of wound healing. Curcumin treatment plays an important anti-inflammatory effect in the process of wound healing. In addition, from the appearance of wound healing and scar formation process, curcumin may also play an important role in the anti-fibroblast collagen synthesis mechanism. The mechanism of treatment to promote wound healing is to prevent the spread of bacteria, control infection, increase blood supply to wounds, improve wound healing microcirculation, promote granular tissue development, reduce gelatin activity, inhibit collagen and gelatin degradation, promote wound healing, and reduce edema reduces vascular permeability. Increased excretion of P and calcitonin is related to local nerve endings, and the expression of endogenous dermal growth factor is affected. Collagen is the main structural and functional protein of skin tissue, which determines its industrial properties, such as

stress intensity. The working principle of collagen in the skin tissue is mainly composed of type I and type III collagen, of which type I collagen is the main body and type III collagen is wrapped in this area, but the reason type III collagen determines the diameter and elasticity of collagen fibers. The higher the content of type III collagen, the thinner the collagen fiber, the better the elasticity, and the lighter the scar, indicating that the ratio of type I and type III collagen is closely related to the quality of repair. The speed of wound healing and the formation of scars are related to the synthesis speed and ratio of type I and II collagen.

Carbon nanotubes have higher tensile strength and modulus, and nano-material bacterial cellulose fibers have higher tensile strength and modulus, and are often added to high-polymer species as a reinforcing agent. From the analysis of TGA and DMA, the addition of carbon nanotubes to the bacterial cellulose fibers to form composite nanomaterials can improve the structural stability and functional modulus of the nanomaterials, indicating that there may be something between carbon nanotubes and bacterial cellulose fibers. This kind of force, the two have a synergistic effect to improve thermal performance and thermomechanical performance. According to this principle, carbon nanotubes should also be able to improve the tensile strength and modulus of composite materials. The slurry formed by the high-speed shearing of the bacterial cellulose fiber through the homogenizer is mixed with the homogeneous suspension of carbon nanotubes and then filtered to form a film. The tensile stress of the composite film that is naturally dried in the air becomes stronger.

Funding

This article is not supported by any foundation.

Data Availability

Data sharing is not applicable to this article as no new data were created or analysed in this study.

Conflict of Interest

The author states that this article has no conflict of interest.

References

- [1] Asadbeigi M, Mirazi N, Vatanchian M, et al. Comparing the healing effect of Lotus Corniculatus Hydroethanolic Extract and phenytoin cream 1% on the rat's skin wound: A Morphometrical and Histopathological Study. *Journal of Chemical and Pharmaceutical Sciences*, 2016, 9(2):746-752.
- [2] Karapolat S, Karapolat B, Buran A, et al. The Effects of Nitrofurazone on Wound Healing in Thoracoabdominal Full-thickness Skin Defects. *WOUNDS A Compendium of Clinical Research and Practice*, 2020, 32(5):134-141.
- [3] Li Y, Wang S, Huang R, et al. Evaluation of the effect of the structure of bacterial cellulose on full thickness skin wound repair on a microfluidic chip. *Biomacromolecules*, 2015, 16(3):780-789. <https://doi.org/10.1021/bm501680s>
- [4] Jimenez F, Poblet E, Izeta A. Reflections on how wound healing-promoting effects of the hair follicle can be translated into clinical practice. *Experimental Dermatology*, 2015, 24(2):91-94. <https://doi.org/10.1111/exd.12521>
- [5] El-Hoseny S M, Basmaji P, Olyveira G M D, et al. Natural ECM-Bacterial Cellulose Wound

- Healing—Dubai Study. *Journal of Biomaterials & Nanobiotechnology*, 2015, 06(4):237-246. <https://doi.org/10.4236/jbmb.2015.64022>
- [6] Peng X, Yu Y, Wang Z, et al. Potentiation effect of HB-EGF on facilitating wound healing via 2-N,6-O-sulfated chitosan nanoparticles modified PLGA scaffold. *RSC Advances*, 2017, 7(68):43161-43171. <https://doi.org/10.1039/C7RA07719J>
- [7] Randy C, Tzi N, Jack W, et al. Chitosan: An Update on Potential Biomedical and Pharmaceutical Applications. *Marine Drugs*, 2015, 13(8):5156-5186. <https://doi.org/10.3390/md13085156>
- [8] Ferenc, Dietrich R, Ganz C, et al. Silicon-dioxidepolyvinylpyrrolidone as a wound dressing for skin defects in a murine model. *Journal of Cranio-Maxillo-Facial Surgery*, 2017, 45(1):99-107.
- [9] Lukanc B, Tončka Potokar, Erjavec V. Observational study of the effect of L-Mesitran® medical honey on wound healing in cats. *Veterinarski Arhiv*, 2018, 88(1):59-74.
- [10] Nezhad M N, Abedian Z, Asili J, et al. Effect of alpha ointment (Fundermol) on episiotomy wound healing in primiparous women. *Iranian Journal of Obstetrics Gynecology & Infertility*, 2017, 20(4):58-65.
- [11] Tomá Komprda. Effect of n-3 long-chain polyunsaturated fatty acids on wound healing using animal models – A review. *Acta Veterinaria Brno*, 2018, 87(4):309-320. <https://doi.org/10.2754/avb201887040309>
- [12] Leonov Y I, Shkumat M S, Klymenko P P, et al. Effect of insulin-like growth factor transgene on wound healing in mice with streptozotocin-induced diabetes. *Cytology & Genetics*, 2015, 49(1):19-26.
- [13] Koo Y, Yun Y. Effects of polydeoxyribonucleotides (PDRN) on wound healing: Electric cell-substrate impedance sensing (ECIS). *Mater, Eng C Mater Biol Appl*, 2016, 69(2):554-560.
- [14] Hai J, Yu L, Xuan L, et al. Healing effect of Shaoshang Yuhe yihao on burns in rats. *Tropical Journal of Pharmaceutical Research*, 2018, 17(2):287-289. <https://doi.org/10.4314/tjpr.v17i2.13>
- [15] Perreault F, Andreia F D F, Elimelech M. Environmental applications of graphene-based nanomaterials. *Chemical Society Reviews*, 2015, 44(16):5861-5896. <https://doi.org/10.1039/C5CS00021A>
- [16] Benck J D, Hellstern T R, Kibsgaard J, et al. Catalyzing the Hydrogen Evolution Reaction (HER) with Molybdenum Sulfide Nanomaterials. *Acs Catalysis*, 2016, 4(11):3957-3971. <https://doi.org/10.1021/cs500923c>
- [17] Shi Y, Zhang B. Correction: Recent advances in transition metal phosphide nanomaterials: synthesis and applications in hydrogen evolution reaction. *Chemical Society Reviews*, 2016, 45(6):1781-1781. <https://doi.org/10.1039/C6CS90013E>
- [18] Shan G, Yan S, Tyagi R D, et al. Applications of Nanomaterials in Environmental Science and Engineering: Review. *Practice Periodical of Hazardous Toxic & Radioactive Waste Management*, 2015, 13(2):110-119.
- [19] Chimene D, Alge D L, Gaharwar A K. Two - Dimensional Nanomaterials for Biomedical Applications: Emerging Trends and Future Prospects. *Advanced Materials*, 2016, 27(45):7261-7284. <https://doi.org/10.1002/adma.201502422>
- [20] Sobon, Grzegorz. Mode-locking of fiber lasers using novel two-dimensional nanomaterials: graphene and topological insulators [Invited]. *Photonics Research*, 2015, 3(2):56-63.
- [21] De Santis E, Ryadnov M G. Peptide self-assembly for nanomaterials: the old new kid on the block. *Chemical Society Reviews*, 2015, 44(22):8288-8300. <https://doi.org/10.1039/C5CS00470E>
- [22] Toma S, Thomas P, Paola A. X-ray photoelectron spectroscopy of graphitic carbon nanomaterials doped with heteroatoms. *Bstn Journal of Nanotechnology*, 2015, 6(1):177-192.

- [23] Ema M, Karin Sørig Hougaard, Kishimoto A, et al. Reproductive and developmental toxicity of carbon-based nanomaterials: A literature review. *Nanotoxicology*, 2016, 10(4):1-22.
- [24] Coll C, Notter D, Gottschalk F, et al. Probabilistic environmental risk assessment of five nanomaterials (nano-TiO₂, nano-Ag, nano-ZnO, CNT, and fullerenes). *Nanotoxicology*, 2015, 10(4):436-444.
- [25] Yu S H, Lee S H, Lee D J, et al. Conversion Reaction - Based Oxide Nanomaterials for Lithium Ion Battery Anodes. *Small*, 2016, 12(16):2146-2172. <https://doi.org/10.1002/sml.201502299>
- [26] Li X, Liu W, Sun L, et al. Effects of physicochemical properties of nanomaterials on their toxicity. *Journal of Biomedical Materials Research Part A*, 2015, 103(7):2499-2507. <https://doi.org/10.1002/jbm.a.35384>
- [27] Pal A K, Bello D, Cohen J, et al. Implications of in vitro dosimetry on toxicological ranking of low aspect ratio engineered nanomaterials. *Nanotoxicology*, 2015, 9(7):871-885. <https://doi.org/10.3109/17435390.2014.986670>